[AMERICAN JOURNAL OF SCIENCE, VOL. 282, FEBRUARY, 1982, P. 136-164]

STABILITY RELATIONS OF THE AMPHIBOLE HASTINGSITE

WARREN M. THOMAS

Department of Earth and Space Sciences, University of California, Los Angeles, California 90024

ABSTRACT. The upper thermal stability limit of the amphibole hastingsite, $NaCa_2Fe_1^{2+}Fe^{3+}Si_6Al_2O_{22}(OH)_2$, has been determined as a function of temperature, fluid pressure, and oxygen fugacity using conventional hydrothermal apparatus and solid oxygen buffers. Dehydration curves were located on the basis of reversals of the reaction

$$\text{hastingsite} \pm xO_2 = \text{anhydrous phases} + H_2O \pm \text{melt}$$

and were found to be constrained by the following P_f-T conditions for the various buffers employed:

	P_f, bars				
Buffer	500	1000	1500	2000	3000
IW	680 ± 15°C	757 ± 8°C	803 ± 8°C	847 ± 5°C	
WM	756 ± 6	840 ± 5	897 ± 6		
FMQ	530 ± 5	616 ± 10		665 ± 5	685 ± 5
NNO	< 505	< 533		< 553	< 557
MH				< 398	

The high-temperature assemblage of equivalent composition consists, with oxygen fugacity defined by the MH buffer, of hematite + grossular-andradite garnet + plagioclase + quartz + magnetite + fluid; by the NNO and FMQ buffers, of hedenbergite + magnetite + plagioclase + grossular-andradite garnet + fluid; by the WM buffer, of hedenbergite + fayalite + magnetite + nepheline + very minor plagioclase + fluid; and by the IW buffer, of hedenbergite + fayalite + nepheline + plagioclase + fluid. Under the oxygen fugacities of the WM buffer, the amphibole dehydration curve intersects the solidus at about 890°C and 1400 bars P_f, above which nepheline is replaced in the product assemblage by a small amount of melt. On isobaric log f_{O_2}-T diagrams, hastingsite has a prow-shaped stability field similar in shape to those of ferropargasite and annite, with the thermal maximum occurring on or near the WM buffer curve. Comparison of the dehydration temperatures for the hornblendes hastingsite and ferropargasite shows a small upward shift of the log f_{O_2}-T stability field for hastingsite, resulting in a slightly higher thermal stability range for this amphibole on FMQ and WM; the average increase at constant P_f is 20°C.

Under IW conditions, for which nepheline is present in the high-temperature assemblage, the addition of excess silica depresses the 2000-bar P_f dehydration temperature by more than 240°C. In contrast, the upper thermal stability of hastingsite on FMQ, for which no undersaturated phase occurs in the product assemblage, is apparently unaffected when hastingsite coexists with quartz.

Refractive indices of synthetic hastingsite are broadly consistent with the endmember values extrapolated from natural hornblendes and vary over the following ranges: n_α = 1.692-1.698 and n_γ = 1.712-1.725, with lower values corresponding to lower oxygen fugacities of synthesis.

Mössbauer spectra were collected and show that the $Fe^{3+}/\Sigma Fe$ ratios vary systematically from 0.116(5) to 0.216(4) for synthetic hastingsites annealed on the IQF and FMQ buffers, respectively. Unit cell parameters, determined by X-ray powder diffraction, indicate that slightly smaller values for a, β, and $a \sin \beta$ correspond to higher Fe^{3+} contents. Representative values for hastingsite synthesized and annealed on the WM buffer and 680°C at $P_f = 3000$ bars are: $a = 9.997(2)$ Å, $b = 18.179(5)$ Å, $c = 5.323(1)$ Å, $\beta = 105.34(2)°$, $a \sin \beta = 9.641(2)$ Å, and $V = 932.9(3)$ Å^3.

Consistent with the experimental results, hastingsite occurs most commonly in nepheline syenites and granites, for some of which a low oxygen fugacity of crystallization has been inferred from independent evidence.

INTRODUCTION

Hornblendes are the most common naturally occurring amphiboles. Chemically complex, their compositions typically must be described in terms of nine or more components. In order to render these minerals more tractable to systematic experimental study, this compositional range may be approximated in terms of a number of simplified compositions, with the natural examples being solid solutions among them. Gilbert (1966) suggested that the sodium-bearing hornblendes be characterized by four such endmembers: pargasite ($NaCa_2Mg_4AlSi_6Al_2O_{22}(OH)_2$), ferropargasite ($NaCa_2Fe_4^{2+}AlSi_6Al_2O_{22}(OH)_2$), magnesiohastingsite ($NaCa_2Mg_4Fe^{3+}Si_6Al_2O_{22}(OH)_2$), and hastingsite ($NaCa_2Fe_4^{2+}Fe^{3+}Si_6Al_2O_{22}(OH)_2$), comprising among them the so-called hornblende quadrilateral (fig. 1). The stability relations of the first three have been previously

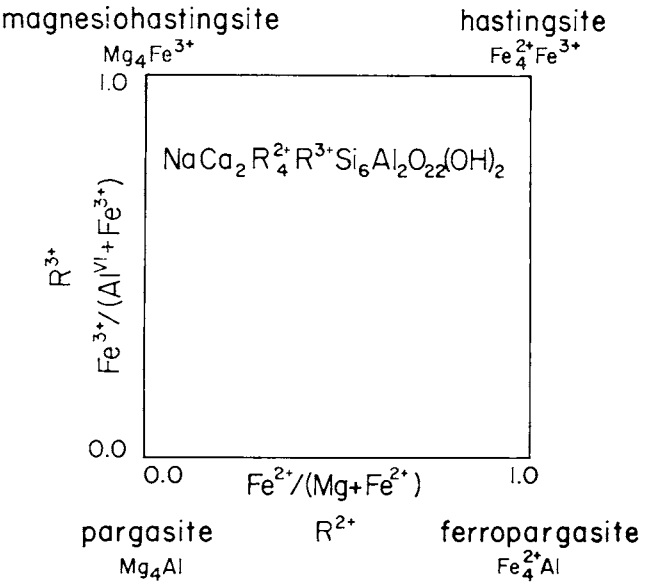

Fig. 1. The hornblende quadrilateral, showing the relationship of the four endmember compositions through two substitutions in the octahedral sites.

determined (Boyd, 1959; Westrich, ms; Gilbert, 1966; Semet, 1970; Semet and Ernst, 1981); the fourth, hastingsite, has been investigated in the present study. Although Colville, Ernst, and Gilbert (1966) first synthesized endmember hastingsite to determine cell parameters and refractive indices, they carried out no systematic investigation of phase relations or changes in properties under different conditions. An investigation of hastingsite stability under the conditions of the graphite-methane buffer, complementary to the present study, was conducted by Charles (1978). Particular interest is attached to the experimental investigation of this hornblende inasmuch as its composition is approached rather closely by many natural specimens, hastingsite and hastingsitic hornblendes being found mainly in granites and feldspathoidal syenites, although occurrences from skarns, gneisses, amphibolites, and schist are also reported (Leake, 1968).

The term hastingsite was first applied by Adams and Harrington (1896) to a ferrous- and ferric-rich, magnesium- and silica-poor hornblende from the nepheline syenite of Dungannon township, Hastings County, Ontario. Since the original description, the term has been used for both paragasite (Berman and Larsen, 1931; Berman, 1937; Hallimond, 1943) and ferropargasite (Smith, 1959), the join between them (Leake, 1968), the entire hornblende quadrilateral excepting endmember pargasite (Whittaker, 1968), as well as the composition under consideration here (Winchell, 1945; Sundius, 1946; Phillips and Layton, 1964; Papike and Cameron, 1976). This last usage has been incorporated in the classification recommended by the International Mineralogical Association's Commission on New Minerals and Mineral Names (Leake, 1978). Unfortunately, the terms hastingsite and ferrohastingsite, used for this composition in Billings' (1928) influential classification, are still frequently used synonymously in the descriptive petrologic literature, although the latter has been marked for formal extinction by the I.M.A. committee. It is the hornblende $NaCa_2Fe_4^{2+}Fe^{3+}Si_6Al_2O_{22}(OH)_2$ that has been investigated in this study and termed hastingsite.

EXPERIMENTAL TECHNIQUES

Conventional cold seal hydrothermal apparatus (Tuttle, 1949) was used for the determination of the hastingsite stability limits. Temperatures were measured using chromel-alumel thermocouples calibrated against the melting points of Zn and NaCl. Water was used as the pressure medium, and pressures were measured with bourdon tube gauges. Temperature fluctuations during an experiment were no more than $\pm$ 3 C°; pressure variations were $\pm$ 10 bars during most runs and never exceeded $\pm$ 30 bars. Oxygen fugacity was controlled using the oxygen buffer technique of Eugster (1957).

Starting materials consisted of an analyzed oxide mix of anhydrous hastingsite composition, synthetic hastingsite or the equivalent anhydrous assemblage synthesized from that mix, or a mixture of hastingsite and anhydrous phases. An approximate ratio of solids to water of 10:1 by

weight was chosen in order to provide water in excess of that required for complete conversion of the charge to amphibole but to minimize the effects of incongruent solubility of the solids in the fluid phase. In addition, two mixes were prepared by the gel method of Hamilton and Henderson (1968); these were of hastingsite and (hastingsite + $3SiO_2$) compositions.

The products of the experiments were examined optically in immersion oils and by X-ray powder diffraction. Cell parameters were determined from X-ray powder diffraction data using MgO (a_0 = 4.2117 Å) as an internal standard and refined using the program of Evans, Appleman, and Handwerker (1963). In all cases, the disaggregated products of the hydrothermal experiments, typically several to several tens of micrometers in longest dimension, are too fine-grained to allow successful mounting and analysis by standard electron microprobe techniques. The products of several experiments, however, were dispersed on flat, polished diamond surfaces and probed qualitatively using an energy dispersive system.

SYNTHETIC PHASES

Hastingsite

The hastingsite synthesized in this study typically occurs as acicular grains having a maximum dimension of 10 μm or less. In some charges crystallized on FMQ (see table 1 for abbreviations), needles up to 30 μm long were observed, but in charges in which nearly complete conversion to amphibole was obtained, the grain size is generally small, and the individual crystals aggregated in large clots. The range of the widths of the crystals is much smaller, from about 1 to 4 μm. The fine grain size and the small number of disaggregated grains suitable for measurement made the determination of the optical properties difficult.

TABLE 1

Abbreviations used in text, tables, and figures.

fay	fayalite
fl	fluid
gar	garnet
hed	hedenbergitic pyroxene
hem	hematite
hst	hastingsite
mag	magnetite
nph	nepheline
plg	plagioclase
qtz	quartz
ss	solid solution
Buffers	
FMQ	fayalite-magnetite-quartz
IQF	iron-quartz-fayalite
IW	iron-wüstite
MH	magnetite-hematite
NNO	nickel-nickel oxide
WM	wüstite-magnetite

The low (n_α) and high (n_γ) refractive indices for four hastingsites synthesized or annealed under oxygen fugacities ranging from IQF to FMQ at P_f(fluid pressure) = 3000 bars and 660 or 680°C were determined in immersion oils. The values of n_α range from 1.692(3) to 1.698(3) and of n_γ from 1.712(3) to 1.725(3); lower values correspond to lower f_{O_2}'s, although the variation is not smooth. The refractive indices of the synthetic hastingsite are consistent with those extrapolated from natural hornblendes, particularly those given by Tröger (1971). In one experiment, the hastingsite euhedra were sufficiently large to observe the absorption and pleochroic scheme: $Z(\gamma) > X(\alpha)$; X = colorless to very pale green, Y = pale green, and Z = olive green to blue green.

^{57}Fe Mössbauer spectra of the synthetic hastingsite are similar to those of natural hornblendes of similar composition. These show that the $Fe^{3+}/(Fe^{2+} + Fe^{3+})$ ratio of the synthetic hastingsite differs from the nominal value of 0.20 and varies systematically as a function of the oxygen fugacity of crystallization and annealing. The lowest value of this ratio, 0.116(5), is for hastingsite annealed on the IQF buffer at 680°C and 3 kb P_f; the highest, 0.216(4), is for hastingsite annealed on FMQ at 660°C and 3 kb P_f. It is thought that the incorporation of extra protons in the amphibole structure may compensate for the charge imbalance caused by the deficiency of ferric iron at low oxygen fugacities, as has been found or inferred in the case of other iron-bearing silicates, including amphiboles (Addison and Sharp, 1962; Kuroda and others, 1975; Semet, 1973, and references contained therein).

Unit cell parameters were determined by X-ray powder diffraction for eight synthetic hastingsites, including those used in the Mössbauer study, as well as for six natural hastingsitic hornblendes. The values for synthetic and natural hornblendes are comparable. Representative cell parameters for hastingsite synthesized and annealed on the WM buffer at 680°C and P_f = 3 kb are: a = 9.997(2) Å, b = 18.179(5) Å, c = 5.323(1) Å, β = 105.34(2) °, $a \sin \beta$ = 9.641(2) Å, and V = 932.9(3) Å^3. (Errors in parentheses are one standard deviation; for 9.997(2) read 9.997 ± 0.002.) Linear least squares fits to plots of each cell parameter versus oxygen fugacity reveal a slight dependence of a, β, and $a \sin \beta$ on oxygen fugacity, with smaller values corresponding to high f_{O_2}'s and hence higher Fe^{3+} contents (Thomas, in preparation). Variation in $a \sin \beta$ reflects the replacement of Fe^{2+} (r = 0.77 Å) by Fe^{3+} (r = 0.64 Å) in the octahedral strip. The range in $Fe^{3+}/(Fe^{2+} + Fe^{3+})$ from 0.12 to 0.22, determined by Mössbauer spectroscopy, suggests a concomitant variation in $a \sin \beta$ of about 0.05 Å; the range actually observed is 0.03 Å. No systematic variation of b, c or V was seen, nor any temperature dependence of any of the parameters observed over the small temperature range investigated (600°-700°C).

Hedenbergite

A hedenbergitic pyroxene is a major phase in the high-temperature assemblage of hastingsite bulk composition under all oxygen fugacities

except those defined by MH, where it is absent, and NNO, where it is much reduced in amount. Bowen, Schairer, and Posnjak (1933) and Rutstein and Yund (1969) gave a value of $n_\gamma = 1.758(3)$ for synthetic endmember hedenbergite ($CaFe^{2+}Si_2O_6$), slightly lower than the range of the indices for the clinopyroxenes ($n_\gamma = 1.761$-1.766) synthesized in this study. Although these indices suggest that the synthetics are of nearly the endmember composition, fortuitous amounts of solid solution with jadeite ($NaAlSi_2O_6$, $n_\gamma = 1.667$, Heinrich, 1965), ferrosilite ($FeSiO_3$, $n_\gamma = 1.794$, Winchell and Winchell, 1951), acmite ($NaFe^{3+}Si_2O_6$, $n_\gamma = 1.836$, Deer, Howie, and Zussman, 1963), and calcium Tschermak's endmember ($CaAlAlSiO_6$, $n_\gamma = 1.730$, Hayes, 1966) could give the same results. The hedenbergitic pyroxene exhibits no apparent variation in n_γ with oxygen fugacity. Likewise, Gilbert (1966) found no change in n_γ for hedenbergitic pyroxene ($n_\gamma = 1.755(5)$ over the range of oxygen fugacities from IW to NNO for the ferropargasite bulk composition; similar insensitivity to oxygen fugacity in synthetic hedenbergite was noted by Rutstein and Yund (1969). In contrast, Ernst (1966) found a systematic increase in the intermediate refractive index (n_β) of hedenbergitic pyroxene that formed in the breakdown assemblage of ferrotremolite (ferroactinolite), an increase that he correlated with increased ferrosilite content. Ernst's n_β value for pure hedenbergite, however, is somewhat lower than Rutstein and Yund's (1969) n_α for the same endmember.

In their studies of pargasite and ferropargasite, Boyd (1959) and Gilbert (1966) postulated that the clinopyroxene in the high-temperature assemblages, diopside and hedenbergite, respectively, must contain some aluminum in order to maintain the appropriate bulk composition. This also seems to be the case for hastingsite, particularly on the WM buffer, where the high-temperature assemblage does not contain enough of the nominally aluminous phases. Qualitative, energy-dispersive microprobe analyses do, in fact, show the presence of aluminum in hedenbergites synthesized on the IW, WM, and FMQ buffers in this study. Furthermore, it is on WM that hedenbergitic pyroxene reaches its maximum and plagioclase its minimum modal amount; the pyroxene evidently contains the aluminum that would otherwise be present in the plagioclase. Similarly, Semet's (ms) microprobe analyses of synthetic diopsidic pyroxenes crystallized in the magnesiohastingsite bulk composition show as many as 0.26 Al atoms per four cation formula unit, most of which can be considered as solid solution toward a Ca- or Mg-Tschermak's endmember.

Magnetite

A magnetite-hercynite spinel is an important phase in the dehydrated condensed assemblage under the oxygen fugacity conditions of the NNO, FMQ, and WM buffers. The bulk composition of the charge constrains the spinel compositions to lie along the magnetite (Fe_3O_4)-hercynite ($FeAl_2O_4$) join. Spinel compositions were determined by the X-ray method of Turnock and Eugster (1962), using Si metal as an internal X-ray standard. The results show that the spinel is very nearly pure magnetite,

with possibly 2 to 3 mole percent hercynite component entering into the spinel synthesized on the WM buffer.

Plagioclase

Plagioclase is found in the hastingsite dehydration assemblage on all buffers used in this investigation, although it occurs in relatively minor amounts on IW and in even smaller quantities on WM. It crystallizes in euhedra up to 0.1 mm in longest dimension and commonly contains abundant inclusions of other phases. The composition of the plagioclase has been inferred from the refractive indices and ranges from $An_{41\pm5}$ on the IW buffer to $An_{28\pm4}$ on the FMQ and NNO buffers. Because nepheline and plagioclase are the only nominally sodium-bearing phases in the hastingsite breakdown assemblages, it is to be expected that the plagioclase would be more calcic in the presence of nepheline on IW and WM and more sodic on FMQ and NNO where nepheline is absent. The surprisingly small amount of plagioclase present on the WM buffer can be explained by the concomitantly large amounts of aluminous hedenbergite, as explained above.

Garnet

A nearly binary grossular (Gro)-andradite (Adr) garnet is an important member of the high-temperature assemblage at the oxidizing conditions of the FMQ, NNO, and MH buffers. The composition of the garnet, which occurs as euhedra or subhedra up to 50 μm in diameter, with some grains showing sector twinning, was obtained by measuring the refractive index and determining the unit cell parameter a_0 from replicate X-ray powder diffraction scans. Owing to the restricted range of compositions possible in this system, these two parameters allow a unique determination using the triangular diagrams of Sriramadas (1957). Garnet compositions range from $Gro_{31}Adr_{69}$ to $Gro_{68}Adr_{32}$, with one determination showing a small amount of almandine component, $Gro_{42}Adr_{53}Alm_5$.

Fayalite

Fayalite is a major member of the high-temperature assemblage on the WM and IW buffers. In this magnesium-free system the only possible deviation from endmember fayalite is limited solid solution toward the calcium-iron olivine, kirschsteinite, $CaFeSiO_4$. Compositions were estimated from the measurement of d_{130}, using the values of 2.8270 Å for fayalite (Fisher and Medaris, 1969) and 2.956 Å for kirschsteinite (Yoder and Sahama, 1957). Assuming a linear relation between this interplanar spacing and composition, probably valid for the small compositional range involved, it can be shown that several fayalites in this study contain about 10 mole percent kirschsteinite component. Cell parameters for one of these fayalites were refined and found to be slightly greater than those of pure fayalite synthesized at 700° and 900°C (Fisher and Medaris, 1969). Inasmuch as the substitution of calcium causes the expansion of the olivine structure (Smith, 1966), it seems reasonable that fayalites synthesized in this study contain a small amount of $CaFeSiO_4$. Finally,

qualitative microprobe analyses show the presence of small amounts of calcium in fayalites synthesized on both the WM and IW buffers.

Nepheline

Nepheline is found in the high-temperature assemblage on the IW and WM buffers. The bulk composition of the charge imposes restrictions on the chemistry of this phase: it must be K-free and thus may show alkali-deficiency and concomitant silica-enrichment by means of the substitution $\square \, Si \rightleftharpoons NaAl$ (Dollase and Thomas, 1978). Qualitative microprobe analyses show the presence of calcium and a small amount of iron. Goldsmith (1949) synthesized nephelines with up to 60 mole percent $CaAl_2O_4$ in solid solution at temperatures as low as 800°C. In addition to the analytical evidence, mass balance considerations suggest that the nepheline in this study, produced at a similar temperature, probably contains around 20 mole percent $CaAl_2O_4$. The iron may be present as Fe^{3+} substituting for tetrahedral Al or as fine magnetite inclusions in the nepheline grains.

Other phases

Other phases encountered include hematite and quartz, both of which are stable in the hastingsite bulk composition under the conditions of the MH buffer. The production of quartz is a result of the instability of hedenbergite under these oxidizing conditions, being replaced by andradite, quartz, and iron oxide(s) (Gustafson, 1974). The composition of the hematite was not determined and is assumed to be pure Fe_2O_3, although up to about 3 wt percent Al_2O_3 may be present in solid solution at 700°C (Turnock and Eugster, 1962).

The presence of a melt in several WM experiments was detected indirectly through the fritted and vesicular appearance of the charge and by the absence of nepheline. In addition, the phases were coarser grained than in the subsolidus runs. The glass itself, however, was difficult to detect optically and is probably present in amounts < 1 percent. Faintly brownish in a few thick shards, it has a refractive index of 1.53(1).

PHASE RELATIONS

Determination of equilibrium

Location of the dehydration curves for hastingsite was accomplished in all cases by determining the direction in which the reaction hastingsite $\pm \, xO_2 =$ anhydrous phases $+ \, H_2O$ proceeded as a function of temperature, fluid pressure, and oxygen fugacity. This was done by observing the crystallization of amphibole from the anhydrous assemblage $+ \, H_2O$ or its dehydration to yield the anhydrous assemblage $+ \, H_2O$, or by noting the increase or decrease in the amount of amphibole relative to product assemblage in mixtures of hastingsite and its high-temperature phase equivalents. This last method, using charges from previous experiments, was the most frequently employed and proved the most useful, inasmuch as it provided information regardless of the direction of the reaction. In some cases such mixtures were rerun several times in order to determine

TABLE 2

Run data for the hastingsite bulk composition + excess H_2O

Run no.	Starting materials	T °C	P_f, bars	Duration, hrs	Results
		IW Buffer			
H358	hed + fay + nph + hst (H356)	650	500	13	(hed + fay + nph) + hst
H364	hed + fay + nph + hst (H362)	666	500	17	(hed + fay + nph) + hst
H374	hed + fay + hst + nph (HS373)	695	500	18	hed + fay + (hst) + nph + plg?
H351	hed + fay + nph + mag + plg? (H349)	730	1000	12	(hed + fay + nph) + hst + (plg)
H354	hed + hst + fay + nph (H353)	740	1000	11½	hst + (hed + fay + nph)
H345	hed + fay + nph (H341)	750	1000	5	hed + fay + nph + hst? + mag?
H352	hed + fay + nph + hst (H348)	760	1000	11½	hed + fay + nph + hst + plg
H367	hed + fay + nph + hst (H365)	767	1000	5½	hed + fay + nph + plg (+ hst)
H359	hed + hst + fay + nph (H354)	782	1000	5	hed + fay + (hst) + nph + plg
H290	hst + hed + fay + nph (H287)	830	1000	6½	hed + fay + plg + nph (+ hst)
H363	hed + fay + nph + hst (H362)	794	1500	6	(hed + fay + nph) + hst (+ plg?)
H365	hed + fay + nph + hst (H363)	795	1500	5	(hed + fay + nph) + hst (+ plg?)
H312	hst + hed + fay + mag (FS272)	810	1500	6	(hst) + hed + fay + nph
H313	hst + hed + fay + mag (FS272)	820	1500	6	(hst) + hed + fay + nph
H335	hed + fay + nph + hst (H334)	820	2000	10	(hed) + hst + (fay + nph)
H337	hed + fay + nph + hst (H336)	829	2000	5	(hed + fay + nph) + hst
H350	hed + fay + nph + hst (H348)	845	2000	4	(hed) + hst + (fay + nph)
H338	hed + fay + nph + hst (H337)	849	2000	4	hed + plg + fay + nph + (hst)
		WM Buffer			
F226	hed + mag + fay + nph (FS220)	725	500	6	(mag + hed + fay + nph) + hst
F214	mag + hed + fay + nph (F211S)	740	500	7	(hed + mag + fay + nph) + hst
F215	hst + mag + hed (F121)	760	500	7	(hst) + hed + mag + fay + nph + plg?
F227	hst + hed + fay + mag + nph? (FS222)	775	500	12	hed + mag + fay + (hst) + nph + plg
F235	hed + mag + fay + nph (FS221)	830	1000	5	(hed + mag + fay + nph) + hst
F245	hed + mag + fay + nph + hst (FS240)	835	1000	8	(hed + mag + fay + nph) + hst
F246	hst + hed + mag + fay + nph (FS242)	845	1000	8	(hst) + hed + mag + fay + nph
F236	hst + hed + mag + fay + nph (FS223)	850	1000	5	hed + (hst) + mag + fay + nph + plg?

F248	hst + hed + mag + fay + nph (FS242)	890	1500	4	hst (+ hed + mag + fay + melt)
F252	hed + mag + fay + nph + plg (FS241)	891	1500	5	hst + (hed + mag + fay + melt)
F249	hst + hed + mag + fay + nph (FS243)	903	1500	5	hed + mag + fay + plg + (hst) + melt
F232	hed + mag + fay + nph (FS221)	830	2000	5	hst + (hed + mag + fay + nph?)
F233	hed + mag + fay + nph (FS221)	850	2000	5	hst + (hed + mag + fay + nph)
F247	hed + mag + fay + nph + hst (FS240)	870	2000	5	hst + (hed + mag + fay + melt)
		FMQ Buffer			
E368	mag + hed + plg + hst (E360)	525	500		768 (mag + hed + plg) + hst + (gar)
E369	mag + hed + plg + hst (E384)	534	500		768 mag + plg + gar + hed
E386	mag + gar + plg + hed + hst (E384)	534	500		577 mag + plg + gar + hed
E371	mag + gar + plg + hed + hst (E361)	545	500		691 mag + plg + gar + hed
E129	hst + mag + hed + plg (E108)	580	1000		288 hst + (mag + plg + hed + gar)
E130	mag + plg + hed + hst + gar (E109)	612	1000		288 hst + (mag + hed + plg + gar)
E254	mag + hed + plg + hst (E205)	618	1000		335 mag + hed + plg + gar + hst
E255	mag + hed + plg + gar + hst (E254)	618	1000		339 mag + hed + plg + gar + hst
E244	hst + hed + fay + mag + nph (FS242)	630	1000		318 (hst) + mag + plg + hed + gar
E174	hst + mag + plg + hed + gar (E130)	640	1000		336 mag + hed + plg + gar (+ hst)
E237	mag + hed + plg + gar + hst (E203)	650	2000		320 hst + (mag + hed + plg + gar)
E238	mag + hed + plg + hst + gar? (E204)	660	2000		320 (mag+) hst + (hed + plg + gar)
E194	hst + hed + mag (FS191)	670	2000		269 mag + (hst) + plg + hed + gar
E175	plg + mag + hed + hst + gar (E135)	680	2000		336 mag + hed + plg + gar + (hst)
E176	hst + mag + hed + plg (E134)	690	2000		336 mag + hed + plg + gar + (hst)
E115	hst + mag + plg + hed + gar (E103)	652	3000		336 hst + (mag + gar)
E116	mag + plg + hed + gar + hst (E106)	680	3000		336 hst + (mag + plg + gar + hst)
E196	hst + hed + mag (FS191)	690	3000		214 mag + (hst) + plg + hed + gar
E261	hst + hed + mag (FS250/1)	697	3000		309 mag + (hst) + hed + plg + gar
E197	hst + hed + mag (FS192)	706	3000		214 mag + plg + hed (+hst) + gar
E178	hst + mag + hed + plg + gar (E105)	710	3000		336 mag + hed + plg + gar + qtz?

Abbreviations are given in table 1; the subscript "ss" (solid solution) has been omitted. All assemblages coexist with fluid. The phases are listed in approximate decreasing order of abundance as estimated from X-ray powder diffraction patterns. Phases enclosed in parentheses are inferred to be metastable by virtue of their decrease relative to the starting materials. Underlining of the abbreviation for hastingsite indicates that the amphibole comprises greater than 90 percent of the charge. Uncertainties in the temperatures are ± 5°C. The run number of experiments whose products were used as the starting materials for a subsequent run are given in parentheses.

unambiguously the direction of the reaction. In some instances these reversed runs provide a tight bracket of ± 5°C for the reaction curve; in others, particularly at low temperatures and fluid pressures, uncertainties are as large as ± 15°C owing to the lack of any observable change in the crystalline mixtures. This tendency for little or no reaction to occur near the curve, especially on the low-temperature side, has been noted by previous workers on amphibole stability, particularly by Boyd (1959) in his study of tremolite. Because hornblendes are compositionally variable, it is possible that the decomposition of hastingsite occurs over a range of temperature, for a given pressure, with a concomitant change in composition over the dehydration interval. The data from this study suggest, however, that such a breakdown range, if it exists, is very narrow and that the corresponding solid solution is limited in composition.

P_f-T diagrams with f_{O_2} defined by oxygen buffers

Dehydration curves were determined for hastingsite using the IW, WM, and FMQ buffers. A summary of the bracketing data is presented in table 2. Complete tables of experimental data for these buffers, as well as for NNO and MH, are to be found in Thomas (ms). Exact modal percentages of minerals in the run products are difficult to estimate inasmuch as the high-temperature phases are present for the most part as aggregates many grains thick. In addition, plagioclase was difficult to detect in runs of short duration on the IW and WM buffers and is listed in table 2 only

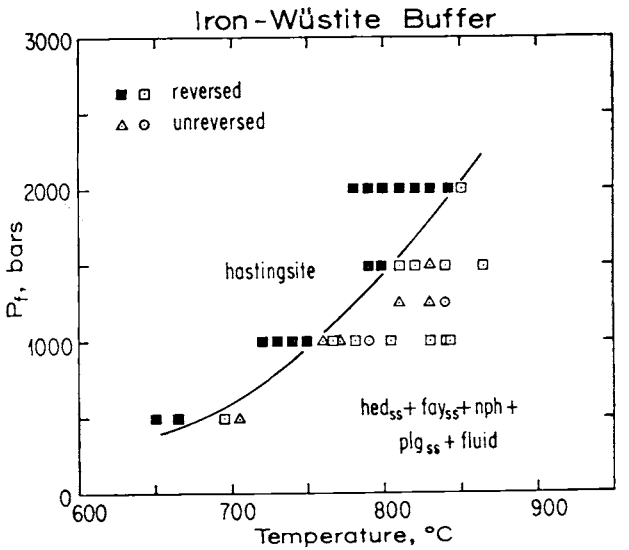

Fig. 2. P_f-T diagram for the hastingsite bulk composition + excess H_2O with oxygen fugacity defined by the IW buffer. Filled squares indicate reversed runs in which hastingsite is stable; open squares reversed runs in which the product assemblage is stable. Open circles represent crystallizations in which the high-temperature assemblage is dominant. Open triangles designate those runs in which the high-temperature assemblage persisted with no detectable decrease.

for runs in which it was unambiguously identified. Balanced reactions can be written for the dehydration of hastingsite, but a unique reaction for each buffer cannot be chosen without accurate compositions for the phases involved.

A. *Iron-wüstite buffer.*—The dehydration curve for hastingsite under the oxygen fugacities imposed by the IW buffer is presented in figure 2. Under these reducing conditions, hastingsite decomposes at: 680 ± 15°C and 500 bars P_f, 757 ± 8°C and 1000 bars, 803 ± 8°C and 1500 bars, and 847 ± 5°C and 2000 bars. The greater uncertainties in temperature at 500 bars is due to the slow rate of reaction and short run durations, together with the shallow slope of the curve, which makes these determinations sensitive to small pressure uncertainties.

The high-temperature assemblage under the investigated P-T conditions consists, in order of decreasing modal abundance, of fayalite, hedenbergite, nepheline, and plagioclase, plus fluid. In addition, an opaque phase is present in quantities much less than one percent and could be minor wüstite contamination from the buffer or magnetite persisting metastably from the initial crystallization of the reduced oxide mix. Optical examination of the high-temperature assemblage before and after rerunning yielded inconclusive evidence on the stability of the opaque phase. In addition, short-duration hastingsite syntheses from the hematite-bearing gel mix did not show metastable magnetite, in contrast to syntheses from the reduced oxide mix. This suggests that the presence of such magnetite is characteristic of charges crystallized from reduced mix. According to the work of Turnock and Eugster (1962), the only Fe-Al spinel that coexists stably with iron and wüstite is very hercynite-rich; in his study of ferropargasite, Gilbert (1966) found a very small amount of spinel in the product assemblage on the IW buffer and inferred it to have such an aluminous composition. The hastingsite bulk composition has one-third less aluminum than ferropargasite, and thus a hercynite-rich spinel would be relatively disfavored in the breakdown products of the former. On the basis of the above evidence, an opaque spinel phase is not considered to be a stable member of the hastingsite product assemblage on the IW buffer. The absence of ferric-bearing phases in the high-temperature assemblage indicates that oxygen is liberated during the dehydration of hastingsite under the conditions of the IW buffer.

B. *Wüstite-magnetite buffer.*—The highest thermal stability found for hastingsite in this study was determined employing the WM buffer. As shown in figure 3, the amphibole breaks down at: 756 ± 5°C and 500 bars P_f, 840 ± 5°C and 1000 bars, and 897 ± 6°C and 1500 bars. Pressure vessel limitations precluded attaining the breakdown temperature at 2000 bars fluid pressure. At 500 and 1000 bars P_f, the high-temperature assemblage consists of hedenbergite, fayalite, magnetite, nepheline, and very minor plagioclase, plus fluid; at 1500 bars, nepheline is absent, and a small amount of melt is present. Based on similar melting of the metastable breakdown assemblage persisting with stable hastingsite in runs at

1500 and 2000 bars, the melting curve has been arbitrarily drawn to intersect the subsolidus dehydration curve at approx 890°C and 1400 bars, a placement that yields the least steep slope for the melting curve allowed by the limited data. The composition of this melt was not determined because of the small amount present. Balanced modal reactions suggest that relatively small amounts of oxygen are involved in hastingsite dehydration on the WM buffer; whether oxygen is liberated or consumed cannot be known without accurate phase compositions and reaction coefficients.

C. *Fayalite-magnetite-quartz- buffer.*—Compared with the results from experiments on the IW and WM buffers, the stability of hastingsite on the FMQ buffer is much reduced. As shown in figure 4, the dehydration curve passes through: 530 ± 5°C and 500 P_f, 616 ± 10°C and 1000 bars, 665 ± 5°C and 2000 bars, and 685 ± 5°C and 3000 bars. At 500 bars, owing primarily to the apparent sluggishness of reaction at these low temperatures and pressure the placement of the lower bracket was based on a subjective judgment that hastingsite had increased in one experiment, albeit very slightly, with increased run durations.

On the FMQ buffer, hedenbergite, magnetite, plagioclase, and an andradite-grossular garnet, plus fluid, comprise the high-temperature assemblage. In contrast to the IW buffer, plagioclase is present in large amounts and is somewhat more sodic. In many buffered synthesis runs

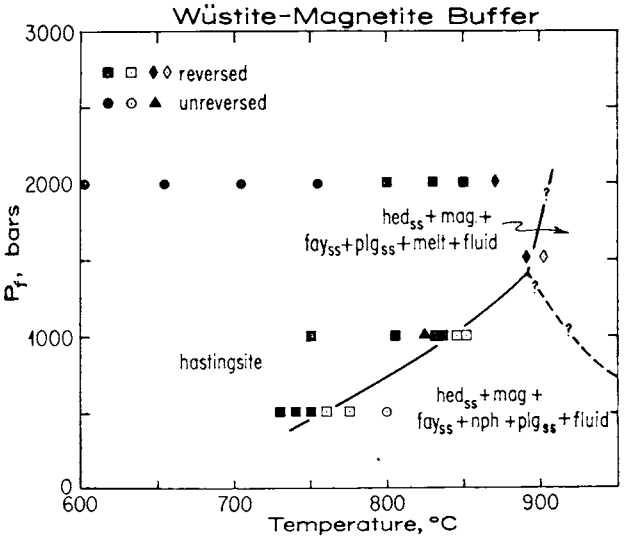

Fig. 3. P_f-T diagram for the hastingsite bulk composition + excess H_2O with oxygen fugacity defined by the WM buffer. Symbols as in figure 2. In addition, the filled circles represent crystallizations from an oxide mix in which hastingsite is present in significant amounts, filled circles designate those runs in which hastingsite persisted with no detectable decrease, the open diamond indicates a reversed run in which the stable high-temperature assemblage contained melt, and the filled diamonds represent reversals in which the metastable product assemblage contained melt.

with the oxide mix as starting material, garnet is present only in minor amounts or is absent even after several hundred hours. With rebuffering and rerunning, garnet increases in amount, both in the stability field of the high-temperature assemblage and in the stability field of hastingsite where decreasing amounts of this high-temperature assemblage persist metastably. Balanced model reactions suggest that, in contrast to the situation for the IW buffer, oxygen is consumed in the dehydration of hastingsite under the conditions of the FMQ buffer.

D. *Nickel-nickel oxide and magnetite-hematite buffers.*—No conclusive demonstration of a stability field for hastingsite was obtained under the conditions of the NNO buffer. Nevertheless, some inferences can be drawn for its probable location. Although hastingsite crystallizes metastably from the reduced oxide mix, sometimes in considerable amounts, on subsequent rerunning it disappears or decreases in amount relative to an assemblage of magnetite, plagioclase, hedenbergite, garnet, and fluid. These observations, together with the partial dehydration of synthetic hastingsite, show that under the conditions of the NNO buffer the upper thermal stability limit must lie below: 505°C at 500 bars P_f, 533°C at 1000 bars, 553°C at 2000 bars, and 557°C at 3000 bars. Attempts to grow amphibole from the high-temperature assemblage at 3000 bars and 528°C and at 2000 bars and both 505 and 526°C were not successful; an experiment using a mixture of anhydrous phases and amphibole showed no change in the amount of the latter after 547 hrs at 3000 bars and 548°C. At these low temperatures, experiments of much longer dura-

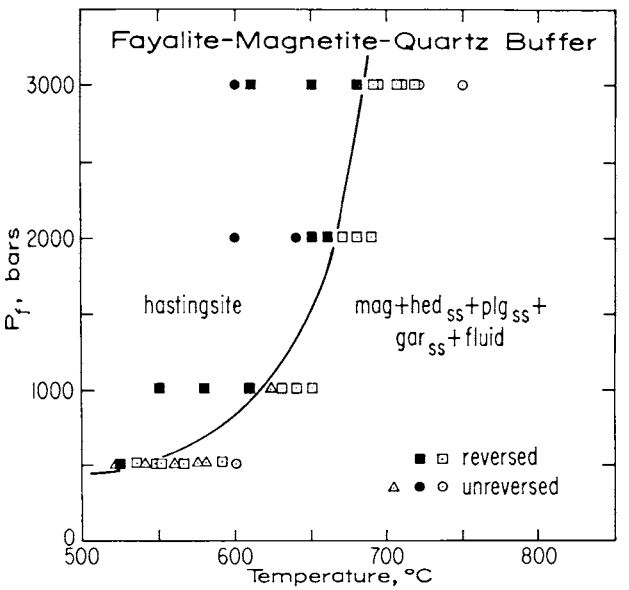

Fig. 4. P_f-T diagram for the hastingsite bulk composition + excess H_2O with oxygen fugacity defined by the fayalite-magnetite-quartz buffer. Symbols as in figures 2 and 3.

tion will be required to locate the hastingsite dehydration curve on this buffer. Consideration of Gilbert's (1966) thermal stability limit for ferropargasite on the NNO buffer and the log f_{O_2}-T curve for hastingsite given below, however, suggests that the curve does not lie more than 30°C below the maximum values given here at pressures greater than a kilobar.

Likewise, no stability field for hastingsite was found for the highly oxidizing conditions of the MH buffer. A series of experiments was conducted at 2000 bars fluid pressure between 398° and 741°C. In all cases the stable assemblage is inferred to be hematite + garnet + plagioclase + quartz + magnetite.

Isobaric log f_{O_2}-T diagrams

Isobaric sections at 1000 and 1500 bars fluid pressure are shown respectively in figures 5 and 6. Owing to the stepwise, discontinuous nature of the control of oxygen fugacity that the solid buffer technique affords, the only points located exactly are those where the equilibrium

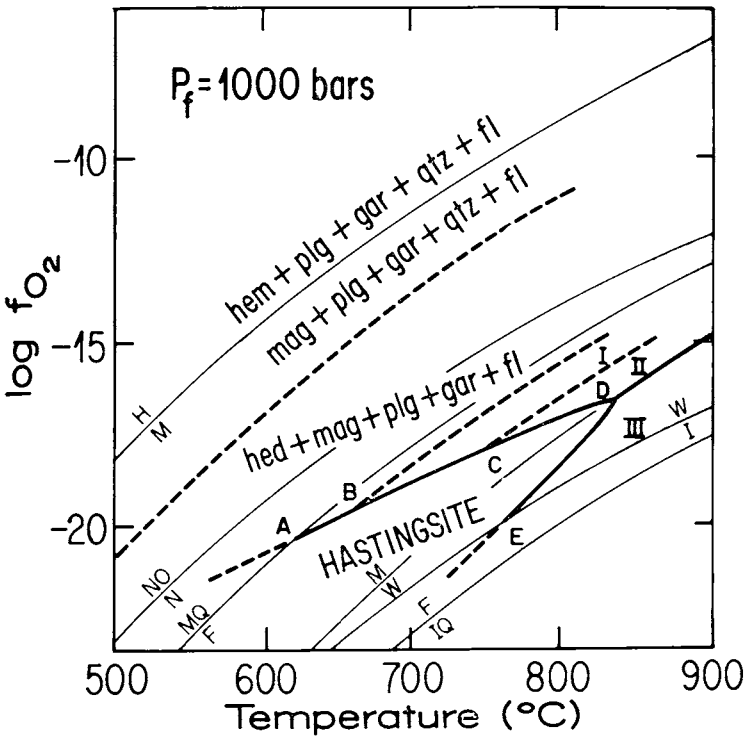

Fig. 5. Isobaric log f_{O_2}-T diagram at P_f = 1000 bars for the hastingsite + excess H_2O bulk composition. Location of points and field boundaries explained in the text. Fields labeled by Roman numerals are for the following assemblages: I: hed + mag + plg + gar + fay + fl; II: hed + fay + mag + nph + plg + fl; and III: hed + fay + nph + plg + fl.

Data for the buffer curves in figures 5, 6, and 8 are from Eugster and Wones (1962) for IW, WM, NNO, and HM and Wones and Gilbert (1969) for FMQ.

curves of interest and the buffer curves intersect. Locations of other points must be inferred and are thus approximate; the associated curves are drawn schematically, consistent with the experimentally determined points.

Figure 5 shows the stability field of hastingsite at P_f = 1000 bars, a prow-shaped region with a shape similar to that for annite (Eugster and Wones, 1962) and ferropargasite (Gilbert, 1966). Points A, D, and E correspond to the dehydration temperature on the FMQ, WM, and IW buffers, respectively. Extrapolation of the hastingsite dehydration curve AD to intersect the NNO curve indicates that the upper thermal stability limit of the amphibole at this pressure is about 525°C consistent with the experimental data described above.

Inasmuch as the high-temperature assemblage is different on the various buffers, a number of reaction curves must be present between these anhydrous assemblages. Between the FMQ and WM buffers, garnet disappears from, whereas fayalite and nepheline appear in, the dehydrated condensed assemblage. This may be accomplished by two or three curves of different variance. In this diagram two curves have been arbitrarily chosen: a fayalite-in and a garnet-out + nepheline-in curve, shown schematically as dashed lines intersecting the hastingsite stability field at points B and C respectively. In accordance with Schreinemaker's

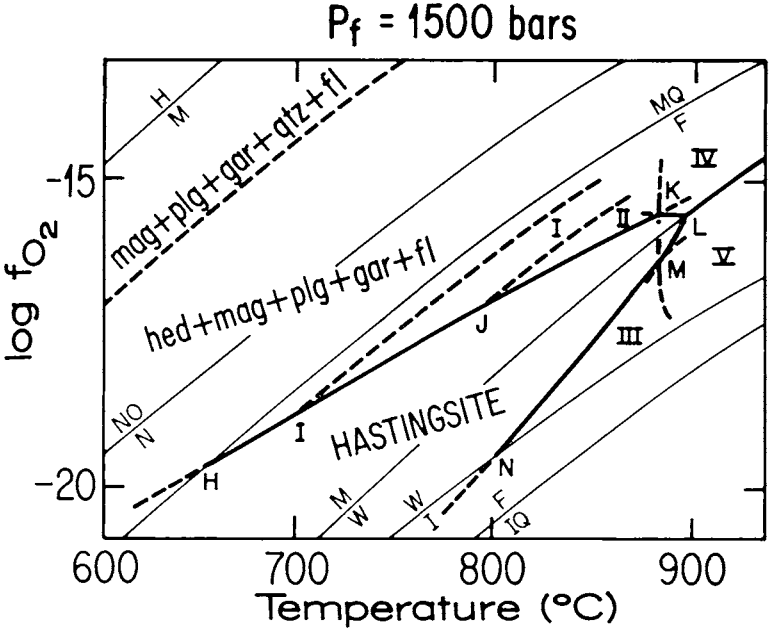

Fig. 6. Isobaric log f_{O_2}-T diagram at P_f = 1500 bars for the hastingsite + excess H_2O bulk composition. Fields I, II, and III are as in figure 10; in addition: IV: hed + fay + mag + plg + melt + fl; and V: hed + fay + plg + melt + fl.

rules, points B and C should mark discontinuities, probably small, in the slope of the isobaric amphibole dehydration curve in log f_{O_2}-T space.

The position of the thermal maximum for the hastingsite field cannot be uniquely determined from the data collected in this study and has been arbitrarily shown to occur on the WM buffer (point D). Alternately, it could lie at the intersection of two hastingsite-out curves and a reaction curve among the anhydrous phases, that is, a higher temperature equivalent of points B or C. Yet another possibility is that it lies between the WM and IW buffer curves on the spinel-out curve for magnetite containing a small amount of hercynite component. If the small hercynite component reported for spinel synthesized on WM is in fact real, then this last possibility may exist. Charles (1978) determined that hastingsite dehydrates at 805°C and 1000 bars P_f on the graphite-methane buffer, that is, at intermediate oxygen fugacities to FMQ and WM. This point is consistent with the curves as drawn here. Additional experiments employing the Co-CoO buffer (Chou, 1978; Myers and Gunter, 1979) might serve to put constraints on the position of the thermal maximum for the hastingsite field.

At 1500 bars P_f, the hastingsite stability extends to high enough temperatures to intersect the solidus for its bulk composition. The presence of melt in the metastable assemblage persisting within the hastingsite field indicates that the amphibole is stable to slightly higher temperatures than the beginning of metastable melting of the anhydrous assemblage. A topology consistent with this interpretation is shown in figure 6; points H, L, and N have been determined experimentally, whereas P, J, K, and M are located schematically. The occurrence of melt on only one buffer provides no control on the slope of the melting curve in this log f_{O_2}-T section. In their study of magnesiohastingsite, Semet and Ernst (1981) found that the solidus for that composition (not the amphibole itself) has an essentially vertical (infinite) slope in the log f_{O_2}-T plot for the range of oxygen fugacities from the MH to the FMQ buffers, indicating little participation of oxygen in the reaction. On the other hand, the beginning of melting of the high-temperature assemblage of riebeckite composition has a positive slope in the log f_{O_2}-T plot at 2000 bars (Ernst, 1962). Lacking the data to fix the slope in the hastingsite system, the melting curve in figure 6 has been drawn independent of oxygen fugacity at moderate f_{O_2} values; a negative slope is conjectured at low f_{O_2}'s where the fugacity of H_2O is reduced.

The effect of excess silica

Owing to the occurrence of hastingsite in quartz-bearing plutonic rocks, it is of interest to investigate the effect of excess silica on the upper thermal stability limit of this hornblende. Accordingly, a number of experiments were conducted using starting mixes of the composition hastingsite + $3SiO_2$, prepared from a gel by the method of Hamilton and Henderson (1968). In each experiment with excess silica, a separate charge of hastingsite bulk composition, also prepared from a gel, was run

in a separate inner capsule inside the same outer capsule as a control. This portion of the investigation is of a reconnaissance nature with a limited number of runs on the IW and FMQ buffers; the results are presented in table 3.

On the IW buffer, all runs were conducted at 2000 bars fluid pressure. Examination of the data shows that, whereas hastingsite is stable to 847 ± 5°C at P_f = 2000 bars on its own bulk composition, the presence of excess silica depresses the decomposition temperature to less than 611°C, below which no reversed experiments were carried out. The high-temperature assemblage of hedenbergite, fayalite, nepheline, and minor plagioclase for the hastingsite bulk composition is replaced in the presence of excess silica by hedenbergite, fayalite, major plagioclase, and minor quartz. Above 675 ± 15°C the silica-rich composition begins to melt, but without the disappearance of any of the solid phases, possibly owing to the small amount of H_2O present in the charge, or by virtue of experimental conditions situated within the plagioclase melting interval.

On the FMQ buffer, amphibole is stable in the presence of quartz at 651°C and P_f = 3000 bars but decomposes at 710°C and P_f = 3000 bars to an assemblage of hedenbergite, plagioclase, fayalite, quartz, magnetite, and fluid. The fact that these runs bracket the 3000-bar dehydration temperature for hastingsite itself, 685 ± 10°C, and average 681 ± 30°C, suggests that the stability of hastingsite under these oxygen fugacities is not much, if any, affected by the presence of quartz.

The stability of hastingsite + $3SiO_2$ on FMQ may serve as a good approximation to this amphibole's stability in fluorine-free granites; here, in contrast to the three other aluminous hornblendes discussed above, it is found naturally with quartz and possesses compositions rather close to the ideal endmember, although a range of compositions toward the more silicic ferroedenite is observed.

The presence or absence of nepheline in the high-temperature assemblage seems to be the most important factor in determining the behavior of hastingsite in the presence of excess silica, and this, in turn, is a function of oxygen fugacity. At low f_{O_2}'s, much or all of the iron is present in ferrous silicates coexisting with nepheline. At higher f_{O_2}'s, the occurrence of Fe in magnetite frees up silica, and no undersaturated silicate phases are present. At the highest f_{O_2}'s investigated (MH buffer), quartz is found in the anhydrous product assemblage of this nepheline-normative amphibole. An analogy may be drawn with the case of the iron biotite, annite. Eugster and Wones (1962) found that for equilibria in which the biotite decomposes to an assemblage containing an undersaturated phase, such as kalsilite or leucite on WM, the upper thermal stability limit is depressed in the presence of quartz, by 120°C at P_f = 2070 bars. For equilibria in which no silica-undersaturated phase is present in the product assemblage, as on HM, NNO, FMQ, and, inferentially, IQF, the dehydration of annite is unaffected by the addition of excess silica.

TABLE 3

Run data for the hastingsite + $3SiO_2$ bulk composition + excess H_2O, as well as hastingsite + excess H_2O control runs, designated by an *.

Run No.	Starting Materials	T, °C	P_f, bars	Duration, hrs	Results
		IW BUFFER			
JH401B	hed + fay + plg + hst + qtz? (JH401)	611	2000	24	hed + fay + plg + qtz? + (hst?)
H402B*	hed + hst + fay + nph + plg? (H402)	611	2000	24	hst + (hed + fay + nph?)
JH423	hed + fay + plg + hst + qtz? (JH405)	630	2000	24	hed + fay + plg + qtz
H424*	hed + fay + hst + plg? (H406)	630	2000	24	hst + (hed + fay + nph?)
JH413	hed + fay + plg + hst + qtz? (JH403)	660	2000	17	hed + fay + plg + qtz?
H414*	hed + fay + hst? + nph? + plg? (H404)	660	2000	17	hst + (hed + fay + nph + plg?)
		FMQ BUFFER			
JE399B	hed + qtz + mag + plg + hst (JE399)	651	3000	223	(hed + plg + qtz + mag) + hst + (fay)
E400B*	hed + mag + plg + gar + hst (E400)	651	3000	223	(hed + plg + mag + gar) + hst (+ fay)
JE425	hed + plg + qtz + mag + hst + fay (JE399)	710	3000	144	hed + plg + fay + qtz + mag

Abbreviations are given in table 1; explanation as in table 2.

COMPARISON OF HORNBLENDE THERMAL STABILITIES

Determination of the hastingsite upper thermal stability limits permits evaluation of the effect of composition on dehydration temperatures of the four aluminous hornblende endmembers (fig. 1). These idealized compositions are related by two substitutions in the octahedral sites: four Fe^{2+} for four Mg, and one Fe^{3+} for one Al. As in the case with many other minerals, the replacement of magnesium by ferrous iron results in a large decline in the upper thermal stability limit, as illustrated by the pairs magnesiohastingsite-hastingsite and pargasite-ferropargasite.

With regard to the Fe^{3+} for Al substitution, the experimental data for amphiboles suggest that the replacement of aluminum by ferric iron elevates the maximum thermal stability under optimal f_{O_2} conditions (Ernst, 1968; Thomas, 1977). In a confirmation of this observation, Semet (1970) found that at low fluid pressures the dehydration curve for magnesiohastingsite under MH conditions is more than 100°C higher than that for pargasite. Under more reducing conditions, however, the decomposition of magnesiohastingsite evolves significant amounts of O_2 and depresses the magnesiohastingsite stability curve below that for pargasite. Clearly then, the effect of the Fe^{3+} for Al substitution is most satisfactorily evaluated in the absence of significant oxidation or reduction of the breakdown assemblage with respect to the amphibole or when similar amounts of O_2 are evolved or consumed in the dehydration of two amphiboles being compared.

A comparison of the dehydration curves for hastingsite and ferropargasite, buffer by buffer, probably approximates this latter criterion and should prove instructive with regard to this substitution. Figure 7 shows the curves for these two amphiboles for the FMQ and WM buffers, respectively. On FMQ, hastingsite dehydrates at a slightly higher temperature than ferropargasite at 1000, 2000, and 3000 bars with the difference becoming less with decreasing fluid pressure; at 500 bars, hastingsite has a lower thermal stability limit than ferropargasite. The reason for this cross-over is not obvious inasmuch as the respective high-temperature assemblages appear to remain the same along the entirety of each curve. For the WM buffer the hastingsite curve similarly lies at higher temperatures than that for ferropargasite. Inspection of the NNO data shows that they too are consistent with a slightly elevated dehydration curve for hastingsite.

Comparison of the data for these two amphiboles on the IW buffer, however, reveals that for $P_f = 500$ and 2000 bars the dehydration temperatures are identical within experimental error, whereas the experimentally determined 1000-bar and the interpolated 1500-bar values for ferropargasite are significantly higher. A log K ($\approx \log f_{H_2O}$)-1/T plot for ferropargasite on IW is, however, nonlinear, suggesting that one of the ferropargasite points may be in error. Although the existence of only three reported points does not permit assessment, by this criterion alone, of which point is incorrect, it has been assumed arbitrarily that the error

resides in the 1000-bar point given by Gilbert (1966) as 800° ± 5°C. By assigning this point a temperature of 775°C, the linearity of the log K-1/T plot is restored, and the P_f-T curve is found to be coincident with that of hastingsite. Because the compositions of the synthetic hastingsite and ferropargasite are different, the coincidence of the two curves is fortuitous; the unexpectedly low values for hastingsite can be explained in an analogous fashion to the relation between magnesiohastingsite under reducing conditions and pargasite: ferric-bearing hastingsite evolves O_2 in its dehydration to an essentially ferric-free high-temperature assemblage, whereas ferric-free ferropargasite evolves no, or possibly consumes small amounts of, O_2 in its decomposition to essentially the same assemblage. (Assignment of the error to either the 500- or 2000-bar point for ferropargasite would result in a corrected curve that would be noncoincident with, and cross, the hastingsite curve.)

Comparison of the stability fields of hastingsite and ferropargasite in a 1000-bar isobaric log f_{O_2}-T section is shown in figure 8. Both are prow-shaped, with that of hastingsite having a slightly higher upper f_{O_2} boundary and probably a higher lower boundary above 750°C. The relative positions of the lower f_{O_2} boundaries will depend on the location of the hastingsite thermal maximum and the dehydration temperature of ferropargasite at 1000 bars P_f on the IW buffer.

In amphiboles, with relatively compliant structures and with a substitution of identically charged and similarly sized octahderally coor-

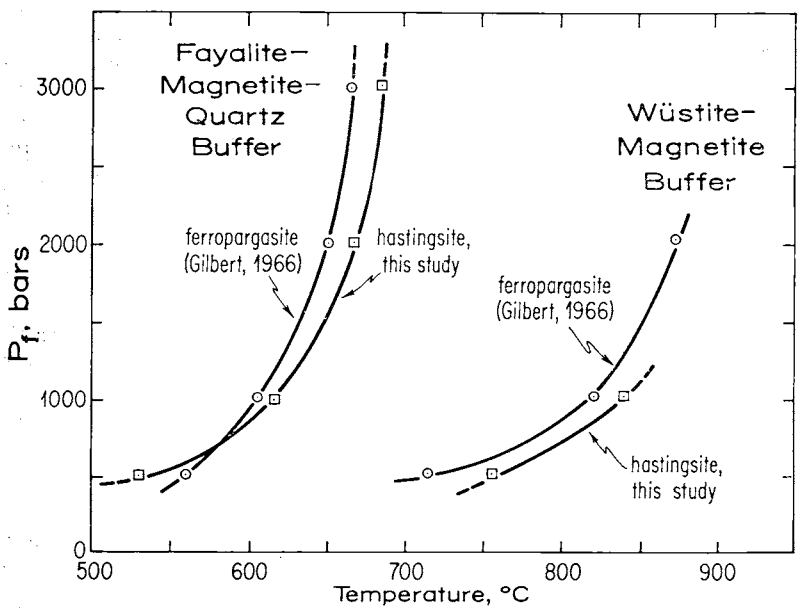

Fig. 7. Comparison of the P_f-T dehydration curves for hastingsite (this study) and ferropargasite (Gilbert, 1966) with oxygen fugacity defined by the WM and FMQ buffers.

dinated cations such as Fe^{3+} and Al (0.64 Å for Fe^{3+} and 0.53 Å for Al, Shannon and Prewitt, 1969), the change in the upper thermal stability limit is most likely to be the result of an absolute change in the free energies of the anhydrous breakdown phases rather than in any inherent stabilization or destabilization of the amphibole with changing composition. Semet and Ernst (1981) have speculated that this results from the apparently greater ease with which Al assumes tetrahedral coordination in the anhydrous phases relative to Fe^{3+}. Finally, it is important to note that, whereas iron-free pargasite is insensitive to f_{O_2} and magnesiohastingsite (Semet and Ernst, 1981) appears to have no high oxygen fugacity limit, hastingsite and ferropargasite are restricted to relatively reducing conditions.

GEOLOGIC APPLICATION

Comparison with natural hornblendes

The compositions of natural hornblendes, when projected into the hornblende quadrilateral, tend to lie in a broad region between hastingsite and pargasite, as shown by Colville, Ernst, and Gilbert (1966). Utilizing the compilation of Leake (1968), Semet and Ernst (1981) demonstrated that a fair number of natural amphiboles also fall in that portion of this diagram near magnesiohastingsite; the region near the ferropargasite composition, however, contains very few natural examples.

In order to survey the compositional variation among the natural hastingsitic hornblendes, analyses were selected from Leake's (1968) cat-

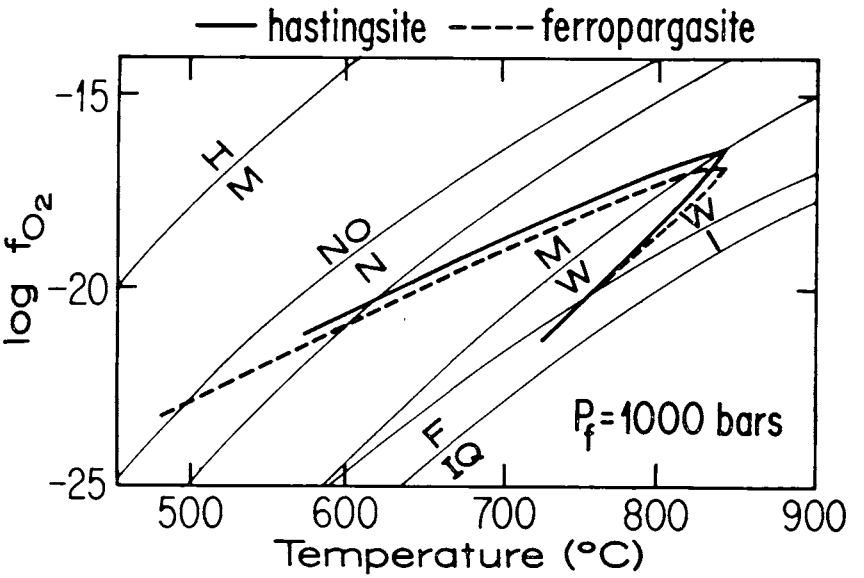

Fig. 8. Comparison of the isobaric log f_{O_2}-T stability fields for hastingsite (this study) and ferropargasite (Gilbert, 1966) at P_f = 1000 bars. The dehydration temperature for ferropargasite on the IW buffer is the adjusted value explained in the text.

alogue, together with all the more recently published values that could be found. All analyses were tabulated with respect to rock type and paragenesis, but only those qualifying as good or superior under Leake's criteria were included when considering chemical variations.

The compositions of natural hastingsitic hornblendes deviate from the ideal endmember, $NaCa_2Fe_4^{2+}Fe^{3+}Si_6Al_2O_{22}(OH)_2$, in a number of ways that cannot be plotted in the hornblende quadrilateral. Chief among these is the continuous ranging of silicon values from less than 6.0 toward 7.0 in more silica-rich ferroedenitic compositions. Calcium reaches the ideal 2 atoms per half unit cell in few specimens, with most values for natural hastingsites being evenly distributed between 1.55 and 2.03. Likewise, Na is usually present in amounts less than 1.0 atom per formula unit, the majority of values ranging from 0.30 to 0.95. In a few cases, however, as many as 1.4 Na atoms may be present. Potassium is invariably present in natural hastingsites, adding a major component not present in the ideal formula or the synthetic system studied here. The ratio K/(K + Na) has a remarkably restricted range of values, with most lying between 0.25 and 0.46 and with a distinct mode at 0.34. The sum (Ca + Na + K), 3.0 in the ideal formula, is generally less in natural samples, ranging evenly from about 2.40 to 3.02. Most hastingsites have < 0.30 Ti/formula unit, with a broad mode at 0.11, a distribution very similar to that given by Leake (1968) for all amphibole analyses with 6.00 to 6.99 Si atoms in the half unit cell.

A significant departure from the ideal hastingsite composition occurs in the substitution of the halogens F and Cl for OH, although evaluation of the prevalence of this replacement is hampered by the scarcity of analyses for these elements. Of the amphiboles considered in this study, 43 percent and 72 percent were not analyzed for F and Cl, respectively. Of those for which these elements were determined, almost all show their presence. Most fluorine values fall evenly distributed between 0.0 and 0.6 with a few extreme values as high as 1.58 per formula unit; chlorine contents also fall between these limits, but with fewer extremely high values. In those hornblendes analyzed for both halogens, fluorine predominates in most igneous occurrences, whereas all but two of the amphiboles in which chlorine predominates are from skarns. This is consistent with the observation (Burnham, 1962; Carmichael, Turner, and Verhoogen, 1974) that fluorine partitions strongly into solid phases relative to a magmatic fluid, whereas chlorine remains in the fluid and escapes unless scapolite is stabilized.

The compositional deviations outlined above will affect the stability relations of natural hastingsitic hornblendes relative to the synthetic endmember studied here. In particular, the substitution of F for OH will raise the amphibole thermal stability relative to the pure hydroxyl endmember, as evidenced by the fact that the one-atm upper thermal stability limit for fluor-tremolite (Comeforo and Kohn, 1954; Troll and Gilbert,

1972; Cameron and Gibbs, 1973) is approx 600°C higher than that for hydroxy-tremolite (extrapolated from Boyd, 1959, by Cameron and Gibbs, 1973). A similar substitution in K-richterite (Gilbert and Briggs, 1974) raises the thermal stability under fluid-absent conditions by as much as 165°C. In addition, Holloway and Ford (1974) found that a 43 percent replacement of the OH by F in pargasite raised the dehydration temperature of that amphibole as well as extending its stability field to higher pressures.

Natural occurrence

Igneous parageneses.—Hastingsite is primarily an amphibole of crustal, perhaps exclusively upper crustal, rocks and is found typically in alkaline igneous intrusives, both undersaturated and oversaturated with respect to silica. The largest number of occurrences are reported from nepheline syenites and granites; quartz-bearing syenites, and calc-alkaline syenites and granodiorites make up the remainder of igneous host rocks, together with one reported occurrence each from a pyroxene peridotite, a diorite, and an albite-nepheline diorite.

Two factors seem to govern the occurrence of hastingsite in igneous rocks, that of bulk composition of the host rock and the oxygen fugacity prevailing at the time of crystallization. Alluminous hornblendes from igneous rocks closely reflect the bulk chemistry of the host rock, particularly with regard to the Fe/(Mg + Fe) ratio. Thus, hastingsite is found in the differentiated, Fe-rich members of alkaline and calc-alkaline plutonic suites (Buddington and Leonard, 1953; Yagi, 1953; Bose, 1964; Frisch, 1970; and Larsen, 1976). Both the experimental evidence and natural occurrences indicate that, in contrast to pargasite and magnesiohastingsite, hastingsite is stable at magmatic temperatures in the presence of quartz at geologically reasonable oxygen fugacities.

The experimental results suggest that the crystallization of hastingsite is favored by low oxygen fugacities. Such an association has been inferred from mineralogical evidence in a number of studies (Bose, 1964; Lyons, 1972; Stull, 1973; Kanisawa, 1975; Larsen, 1976). Lyons, for example, concluded that the presence of hastingsite in the Peabody granite of New England and of riebeckite in the neighboring, and coeval, Quincy granite is the result of both contrasting bulk composition chemistries and disparate values of f_{O_2} (see also Ernst, 1962). Aegerine, magnetite, and traces of hematite occur in the Quincy granite, as well as hematite (+ magnetite?) in an associated pegmatite (Warren and Palache, 1911), whereas of these only magnetite is found in the Peabody granite. In addition, a europium depletion in the feldspar of the Quincy granite (Buma, Frey, and Wones, 1971) suggests that crystallization under high oxygen fugacities resulted in Eu^{3+} rather than Eu^{2+}, the former not entering the feldspar structure as readily as the latter (Drake, 1975; Drake and Weill, 1975). Ernst (1962) suggested that higher oxygen fugacities favor riebeckite and lower f_{O_2} favors either arfvedsonite or hastingsite, depending on the Na/Ca ratio in the host rock. Slightly higher values for this ratio will

favor arfvedsonite coexisting with a sodic plagioclase (An_{10}, for example), whereas lower values will favor hastingsite + slightly more calcic plagioclase associations.

The scarcity of ferropargasite and relative abundance of hastingsite in intrusive rocks was ascribed by Gilbert (1966) to the probable increased stability of endmember hastingsite under higher fugacities of oxygen relative to endmember ferropargasite. The present study has shown that, although hastingsite is stable to slightly higher oxidation states, the magnitude of the effect is not large. Nonetheless, because the stability fields of both these hornblendes are at the lower limit of what is generally regarded as the range of geologically probably oxygen fugacities (see Carmichael, Turner, and Verhoogen, 1974), even small f_{O_2} differences may result in many more occurrences of hastingsite. Differences in bulk composition may also be important. The stability fields determined experimentally are those of the amphiboles on their own bulk compositions, for which their stabilities are at a maximum. In the presence of other components, more aluminous ferropargasite may be metastable with respect to an assemblage containing other aluminum-bearing phases, such as feldspar or a feldspathoid.

Metamorphic parageneses.—Metamorphic hastingsites are far less abundant than those from igneous parageneses, and most have been found in skarns, with gneisses and amphibolites being the next most common host rocks. Less common occurrences include calcite marble, charnockite, granulite, a hornblendite, and a hastingsite schist.

Although the number of analyses is small and perhaps unrepresentative, the apparent correlation between chlorine content and metamorphic occurrence is striking. Of the thirteen published analyses in which chlorine predominates over fluorine, ten are from skarns of seven different localities, and the eleventh is from the hastingsite schist; the two remaining are from igneous parageneses. On the other hand, of those analyses in which fluorine is more abundant than chlorine, only one is from a skarn, two are from granite gneisses, and the remaining nine from igneous intrusives.

Chlorine-bearing metamorphic hastingsites occur in calc-silicate skarns (Matsumoto, 1968, 1969; Matsumoto and Miyahisa, 1960) in a sphalerite-bearing skarn (Dick and Robinson, 1979), and in a number of magnetite-bearing skarn deposits, some apparently of commercial grade (Krutov, 1936; Krutov and Vinogradova, 1966).

That chloramphiboles may not be stable at magmatic temperatures is suggested by the work of Huebner and Papike (1970); those authors found that hydroxyl-richterite does not take up detectable Cl from (Na,K)Cl melts at 850°C and 1000 bars. The presence of chlorine in metamorphic hastingsite, then, may be the result of their lower temperature of crystallization or a very specific chemical environment (Malinovsky, 1966, 1967; Dick and Robinson, 1979).

SUMMARY

The results of this experimental study of the stability of hastingsite are consistent with, and elucidate, several important aspects of the natural occurrence of this amphibole. First, the crystallization of hastingsite is restricted to relatively low oxygen fugacities. Second, hastingsite is stable in the presence of quartz at the geologically reasonable oxygen fugacities of the FMQ buffer, and perhaps somewhat lower. Third, pure hydroxyl-hastingsite is stable at magmatic temperatures only above 3000 bars fluid pressure under FMQ oxygen fugacities but at fluid pressures as low as 500 bars under IW and WM conditions.

Some caution must be exercised in the quantitative application of the results obtained in this study to natural occurrences. The stabilities determined here for the pure hydroxyl-bearing endmember are not strictly applicable to natural hornblendes characterized by the presence of additional components not included in the experimental system. Among these, the effects of Mg and F are known: both result in the raising of the thermal stability relative to the values determined here. The presence of these elements, even in small amounts, and probably also K (see Helz, 1979), expands the stability field of natural hastingsitic hornblendes to magmatic temperatures at lower fluid pressures under higher f_{O_2} values (FMQ or higher) and possibly in the presence of quartz at very low oxygen fugacities equivalent to the IW and WM buffers.

ACKNOWLEDGMENTS

This paper is based on the author's Ph.D. dissertation submitted to the University of California, Los Angeles. The guidance and support of W. G. Ernst is gratefully acknowledged. For their useful discussions during the course of the study, the author would like to thank W. A. Dollase, J. L. Rosenfeld, W. D. Carlson, F. S. Spear, and G. A. Waychunas. A preliminary draft was reviewed by W. G. Ernst and W. A. Dollase; a revised version benefited from the helpful criticism of R. W. Charles. This study was supported by NSF grant EAR 77-10649/Ernst.

REFERENCES

Adams, F. D., and Harrington, B. J., 1896, On a new alkali hornblende and a titaniferous andradite from the nepheline-syenite of Dungannon, Hastings County, Ontario: Am. Jour. Sci., 4th ser., v. 1, p. 210-218.

Addison, W. E., and Sharp, J. H., 1962, Amphiboles. Part III. The reduction of crocidolite: Chem. Soc. Jour., p. 3693-3698.

Berman, H., 1937, Constitution and classification of the natural silicates: Am. Mineralogist, v. 22, p. 342-408.

Berman, H., and Larsen, E. S., 1931, Composition of the alkali amphiboles: Am. Mineralogist, v. 16, p. 140-144.

Billings, M. P., 1928, The chemistry, optics and genesis of the hastingsite group of amphiboles: Am. Mineralogist, v. 13, p. 287-296.

Bose, M. K., 1964, Amphiboles in alkaline rocks of Karaput, Orissa: Mineralog. Mag., v. 33, p. 912-917.

Bowen, N. L., Schairer, J. F., and Posnjak, E., 1933, The system CaO-FeO-SiO_2: Am. Jour. Sci., 5th ser., v. 29, p. 151-217.

Boyd, F. R., 1959, Hydrothermal investigations of amphiboles, *in* Abelson, P., ed., Researches in Geochemistry: New York, John Wiley & Sons, p. 377-396.

Buddington, A. F., and Leonard, B. F., 1953, Chemical petrology and mineralogy of hornblendes in northwest Adirondack granitic rocks: Am. Mineralogist, v. 38, p. 891-902.

Buma, G., Frey, F. A., and Wones, D. R., 1971, New England granites: Trace element evidence regarding their origin and differentiation: Contr. Mineralogy Petrology, v. 31, p. 300-320.

Burnham, C. W., 1962, Hydrothermal fluids at the magmatic stage, *in* Barnes, H. L., ed., Geochemistry of Hydrothermal Ore Deposits: New York, Holt, Reinhart, and Winston, p. 34-76.

Cameron, M., and Gibbs, G. V., 1973, The crystal structure and bonding of fluor-tremolite: A comparison with hydroxyl tremolite: Am. Mineralogist, v. 58, p. 879-888.

Carmichael, I. S. E., Turner, F. J., and Verhoogen, J., 1974, Igneous Petrology: New York, McGraw-Hill, 739 p.

Charles, R. W., 1978, Synthesis and stability of hastingsite: $Ca_2NaFe_4Fe^{3+}Si_6Al_2O_{22}(OH)_2$ [abs.]: Am. Geophys. Union Trans., v. 59, p. 1217.

Chou, I-M., 1978, Calibration of oxygen buffers at elevated P and T using the hydrogen fugacity sensor: Am. Mineralogist, v. 63, p. 690-703.

Colville, P., Ernst, W. G., and Gilbert, M. C., 1966, Relationships between cell parameters and chemical compositions of monoclinic amphiboles: Am. Mineralogist, v. 51, p. 1727-1754.

Comeforo, J. E., and Kohn, A. J., 1954, Synthetic asbestos investigations. I. Study of synthetic fluor-tremolite: Am. Mineralogist, v. 39, p. 537-548.

Deer, W. A., Howie, R. A., and Zussman, J., 1963, Rock Forming Minerals. V. 2. Chain Silicates: London, Longmans, 379 p.

Dick, L. A., and Robinson, G. W., 1979, A chlorine-bearing potassian hastingsite from a sphalerite skarn in southern Yukon: Canadian Mineralogist:, v. 17, p. 25-26.

Dollase, W. A., and Thomas, W. M., 1978, The crystal chemistry of silica-rich, alkali-deficient nepheline: Contr. Mineralogy Petrology, v. 66, p. 311-318.

Drake, M. J., 1975, The oxidation state of europium as an indicator of oxygen fugacity: Geochim. et Cosmochim. Acta, v. 39, p. 55-64.

Drake, M. J., and Weill, D. F., 1975, Partition of Sr, Ba, Ca, Y, Eu^{2+}, Eu^{3+}, and other REE between plagioclase feldspar and magnatic liquid: Geochim. et Cosmochim. Acta, v. 39, p. 689-712.

Ernst, W. G., 1962, Synthesis, stability relations, and occurrence of riebeckite and riebeckite-arfvedsonite solid solutions: Jour. Geology, v. 70, p. 689-736.

———— 1966, Synthesis and stability relations of ferrotremolite: Am. Jour. Sci., v. 264, p. 37-65.

———— 1968, Amphiboles: New York, Springer-Verlag, 125 p.

Eugster, H. P., 1957, Heterogeneous reactions involving oxidation and reduction at high pressures and temperatures: Jour. Chem. Physics, v. 26, p. 1760-1761.

Eugster, H. P., and Wones, D. R., 1962, Stability relations of the ferruginous biotite, annite: Jour. Petrology, v. 3, p. 82-115.

Evans, H. T., Jr., Appleman, D. E., and Handwerker, D. S., 1963, The least-squares refinement of crystal unit cells with powder diffraction data by an automatic computer indexing method [abs.]: Am. Cryst. Assoc., Cambridge, Mass., Annu. Mtg. Program, p. 42-43.

Fisher, G. W., and Medaris, L. G., Jr., 1969, Cell dimensions and x-ray determinative curve for synthetic Mg-Fe olivines: Am. Mineralogist, v. 54, p. 741-753.

Frisch, T., 1970, Chemical variations among the amphiboles of Shefford Mountain, a Monteregian intrusion in southern Quebec: Canadian Mineralogist, v. 10, p. 553-570.

Gilbert, M. C., 1966, Synthesis and stability relations of the hornblende ferropargasite: Am. Jour. Sci., v. 264, p. 698-742.

Gilbert, M. C., and Briggs, D. F., 1974, Comparison of the stabilities of OH- and F-potassic richterites — A preliminary report [abs.]: Am. Geophys. Union Trans., v. 55, p. 480.

Goldsmith, J. R., 1949, Some aspects of the system $NaAlSiO_4$–$CaO \cdot Al_2O_3$: Am. Mineralogist, v. 34, p. 471-493.

Gustafson, W. I., 1974, The stability of andradite, hedenbergite and related minerals in the system Ca-Fe-Si-O-H: Jour. Petrology, v. 15, p. 455-496.

Hallimond, A. F., 1943, On the graphical representation of the calciferous amphiboles: Am. Mineralogist, v. 28, p. 65-89.

Hamilton, D. L., and Henderson, C. M. B., 1968, The preparation of silicate compositions by a gelling method: Mineralog. Mag., v. 36, p. 832-838.

Hayes, J. F., 1966, Stability and properties of the synthetic pyroxene $CaAl_2SiO_6$: Am. Mineralogist, v. 51, p. 1524-1528.

Heinrich, E. W., 1965, Microscopic Identification of Minerals: New York, McGraw-Hill, 414 p.

Helz, R. T., 1979, Alkali exchange between hornblende and melt: a temperature-sensitive reaction: Am. Mineralogist, v. 64, p. 953-965.

Holloway, J. R., and Ford, C. E., 1974, Fluid-absent melting of the fluorhydroxy amphibole paragasite to 35 kilobars: Earth Planetary Sci. Letters, v. 25, p. 44-48.

Huebner, J. S., and Papike, J. J., 1970, Synthesis and sodium-potassium exchange in the richterite series $(K,Na)NaCaMg_5Si_8O_{22}(OH)_2$ [abs.]: Am. Mineralogist, v. 55, p. 300-301.

Kanisawa, S., 1975, Chemical composition of hornblendes of some Ryoke granites, central Japan: Japan Assoc. Mineralogy Petrology Econ. Geology Jour., v. 70, p. 200-211.

Krutov, A., 1936, Dashkessanite — a new chlorine amphibole of the hastingsite group: Acad. Sci. USSR Bull. Cl. Sci. Mat. Nat., Ser. Geol., p. 341-371 (p. 371-373, English summary).

Krutov, G. A., and Vinogradova, R. A., 1966, Chlorohastingsites from the Odinochnoye magnetite deposit, eastern Sayan: Acad. Sci. USSR Doklady, Earth Sci. Sec., v. 169, p. 116-119.

Kuroda, Y., Hariya, Y., Suzuoki, T., and Matsuo, S., 1975, Pressure effect on water content of amphiboles: Geophys. Research Letters, v. 2, p. 529-531.

Larsen, L. M., 1976, Clinopyroxenes and coexisting mafic minerals from the alkaline Ilimaussaq intrusion, south Greenland: Jour. Petrology, v. 17, p. 258-290.

Leake, B. E., 1968, A catalogue of analyzed calciferous and subcaliferous amphiboles together with their nomenclature and associated minerals: Geol. Soc. America Spec. Paper 98, 210 p.

———— 1978, Nomenclature of amphiboles: Canadian Mineralogist, v. 16, p. 501-520.

Lyons, P. C., 1972, Significance of riebeckite and ferrohastingsite in microperthite granites: Am. Mineralogist, v. 57, p. 1404-1412.

Malinovskiy, I. Yu, 1966, Hydrothermal synthesis of amphibole of the ferroedenite-ferrohastingsite series: Akad. Nauk SSSR Doklady, Earth Sci. Sec., v. 170, p. 164-166.

———— 1967, Hydrothermal synthesis of iron cordierite in experiments on the synthesis of ferrohastingsite: Akad. Nauk SSSR Doklady, Earth Sci. Sec., v. 173, p. 114-115.

Matsumoto, Y., 1968, Ferrohastingsite from the Kinbu mine, Nagano Prefecture, Japan: Nagasaki Univ. Fac. Liberal Arts Bull., Nat. Sci., v. 8, p. 39-46.

———— 1969, Ferrohastingsite from the Moji mine, Fukuoka Prefecture, Japan: Sci. Rept., Kyushu Univ. Fac. Sci., Geol. Sci. Rept., v. 9, p. 1-7.

Matsumoto, Y., and Miyahisa, M., 1960, Ferrohastingsite from the Obira mine, Kyushu, Japan: Mineralog. Soc. Japan Jour., v. 4, p. 372-382.

Myers, J., and Gunter, W. D., 1979, Measurement of the oxygen fugacity of the cobalt-cobalt oxide buffer assemblage: Am. Mineralogist, v. 64, p. 224-228.

Papike, J. J., and Cameron, M., 1976, Crystal chemistry of silicate minerals of geophysical interest: Rev. Geophysics Space Physics, v. 14, p. 37-78.

Phillips, R., and Layton, W., 1964, The calciferous and alkali amphiboles: Mineralog. Mag., v. 33, p. 1097-1109.

Rutstein, M. S., and Yund, R. A., 1969, Unit cell parameters of diopside-hedenbergite solid solutions: Am. Mineralogist, v. 54, p. 238-245.

Semet, M. P., 1970, Stability relations of the amphibole magnesiohastingsite [abs.]: Am. Mineralogist, v. 55, p. 311-312.

———— ms, 1972, Stability relations and crystal chemistry of the amphibole magnesiohastingsite, $NaCa_2Mg_4Fe^{3+}Si_6Al_2O_{22}(OH)_2$: Ph.D. dissert., Univ. California, Los Angeles, 216 p.

———— 1973, A crystal-chemical study of synthetic magnesiohastingsite: Am. Mineralogist, v. 58, p. 480-494.

Semet, M. P., and Ernst, W. G., 1981, Experimental stability relations of the hornblende magnesiohastingsite: Geol. Soc. America Bull., pt. 2, p. 274-357.

Shannon, R. D., and Prewitt, C. T., 1969, Effective ionic radii in oxides and fluorides: Acta Cryst., v. B25, p. 925-946.

Smith, J. V., 1959, Graphical representation of amphibole compositions: Am. Mineralogist, v. 44, p. 437-440.

———— 1966, X-ray emission microanalysis of rock-forming minerals. II. Olivines: Jour. Geology, v. 74, p. 1-16.

Sriramadas, A., 1957, Diagrams for the correlation of unit cell edges and refractive indices with the chemical composition of garnets: Am. Mineralogist, v. 42, p. 294-298.

Stull, R. J., 1973, Calcic and alkali amphiboles from the Golden Horn batholith, North Cascades, Washington: Am. Mineralogist, v. 58, p. 873-878.

Sundius, N., 1946, The classification of the hornblendes and the solid solution relations in the amphibole group: Sveriges Geol. Undersökning, v. 40, no. 4, 36 p.

Thomas, W. M., 1977, Preliminary stability relations of the hornblende hastingsite, and the effect of Fe^{3+} for aluminum replacement in amphiboles [abs.]: Am. Geopys. Union Trans., v. 58, p. 1244.

———— ms, 1979, Stability relations of the amphibole hastingsite, $NaCa_2Fe_4^{2+}Fe^{3+}Si_6Al_2O_{22}(OH)_2$: Ph.D. dissert., Univ. California, Los Angeles, 183 p.

Tröger, W. E., 1971, Optische Bestimmung der gesteinsbildenden Minerale, Teil I, 4. Auflage: Stuttgart, E. Schweizerbart'sche Verlagsbuchhand., 147 p.

Troll, G., and Gilbert, M. C., 1972, Fluorine-hydroxyl substitution in tremolite: Am. Mineralogist, v. 57, p. 1386-1403.

Turnock, A. C., and Eugster, H. P., 1962, Fe-Al oxides: phase relationships below 1000°C: Jour. Petrology, v. 3, p. 533-565.

Tuttle, O. F., 1949, Two pressure vessels for silicate-water studies: Geol. Soc. America Bull., v. 60, p. 1727-1729.

Warren, C. H., and Palache, C., 1911, The pegmatites of the riebeckite-aegerite granite of Quincy, Mass., USA: their structure, minerals, and origin: Am. Acad. Arts Sci. Proc., v. 47, p. 125-168.

Westrich, H. R., ms, 1978, Fluoride-hydroxyl exchange equilibria in several hydrous minerals: Ph.D. dissert., Arizona State Univ., 152 p.

Whittaker, E. J. W., 1968, Classification of the amphiboles, *in* Internat. Mineralog. Assoc. Proc., 5th General Mtg. 1966: London, Mineralog. Soc., p. 232-242.

Winchell, A. N., 1945, Variations in composition and properties of the calciferous amphiboles: Am. Mineralogist, v. 30, p. 27-50.

Winchell, A. N., and Winchell, H., 1951, Elements of Optical Mineralogy. Part II. Descriptions of Minerals: New York, John Wiley & Sons, 551 p.

Wones, D. R., and Gilbert, M. C., 1969, The fayalite-magnetite-quartz assemblage between 600° and 800°C: Am. Jour. Sci., v. 267-A, p. 480-488.

Yagi, K., 1953, Petrochemical studies on the alkalic rocks of the Morotu district, Sakhalin: Geol. Soc. America Bull., v. 64, p. 769-809.

Yoder, H. S., Jr., and Sahama, T. G., 1957, Olivine x-ray determinative curve: Am. Mineralogist, v. 42, p. 475-491.